Electroanalytical metal sensor with built-in oxygen filter

Elise Rotureau, Julius Gajdar, Grégoire Herzog, Yves Waldvogel, José-Paulo F Pinheiro, M. Etienne

Electroanalytical metal sensor with built-in oxygen filter

Elise Rotureau,[a] Julius Gajdar,[b,c] Grégoire Herzog,[b] Yves Waldvogel [a], José-Paulo Pinheiro,[a] Mathieu Etienne[b,*]

[a] Université de Lorraine and CNRS, LIEC, UMR7360, Nancy, France

[b] CNRS and Université de Lorraine, LCPME, UMR7564, Nancy, France

[c] SATT Sayens, Nancy, France

Abstract

A rapid and reliable oxygen elimination system was evaluated here for the electroanalytical study of metals. Dissolved oxygen was removed locally in the vicinity of a sensor by the means of electrochemical oxygen filter constructed from platinum grids. Three metals (Cd, Pb, and Zn) were determined by stripping chronopotentiometry (SCP) at a mercury film screen-printed electrode. Limits of detection of metals were in the nanomolar range under optimized experimental conditions. The electrochemical device was also tested for metal quantification in simple electrolyte solutions and in a natural water matrix. The proposed combination of oxygen elimination system with the metal sensor completely removes the need to purge the sample before SCP measurement. This makes the determination of metals by SCP faster, portable and more suited for on-field applications.

Highlights:

- Electrochemical oxygen filter is combined with a metal sensing system
- Stripping chronopotentiometry is accordingly adapted for the optimal filter use
- Comparable limits of detection are obtained with O_2 filter and classical N_2 purging
- Total metal concentration is quantified for different matrix solutions

Keywords: Trace metals, detection, electrochemical oxygen filter, stripping chronopotentiometry, portable device

1. Introduction

Detection and monitoring of trace amounts of metals is paramount for assessing the quality of water, soil, food, etc. While some metals are essential to life in small quantities, they can be toxic at higher concentrations. Additionally, heavy metals (such as lead, cadmium, etc.) are a hazard to the environment and the human health even at trace concentration levels [1,2]. Therefore, there is an interest in the development of highly selective, sensitive and easy-to-use analytical methods and measurement protocols for the determination of metals in complex matrices and for their application in on-field devices [3].

Generally, techniques like atomic absorption spectroscopy (AAS) or inductively coupled plasma mass spectrometry (ICP-MS) are favourably employed for the detection of metals in complex matrices [4,5]. These techniques are able to achieve very low detection limits, down to femtomolar range in some studies [6]. However, these techniques usually require expensive, bulky and complicated instrumentation not suitable for on-field operations. Another group of techniques used for the sensitive determination of metals are electrochemical techniques. Contrary to spectrometric techniques, they are low-cost, user-friendly, easily portable and therefore suited for on-site applications [3]. The most commonly used techniques for trace metal detection are employing a deposition of metals onto the electrode surface at a given potential. The accumulated metal is then stripped by employing either a voltammetric or a galvanostatic technique. The most sensitive voltammetric techniques that follow the deposition step are differential pulse (DPV) or square-wave voltammetry (SWV) [3,7,8]. Use of galvanostatic technique such as stripping chronopotentiometry (SCP) offers a few advantages over voltammetric techniques. SCP can be used as a robust method for analysis of the dynamic of metal speciation [9,10] and, additionally, it was proven to be less sensitive to the presence of organic matter in a sample.[11] It can also provide speciation information in relation to the studied metal [8]. Recently, SCP has been employed in a speciation analysis of indium [12], determination of metals in beverages [13] or determination of zinc in freshwaters [14].

One of the major problems in SCP experiments is its high sensitivity to dissolved oxygen. Therefore, the solutions must be purged with nitrogen usually for at least 20 mins, which is difficult under the field conditions [15,16]. A previous study [17] tackled this issue by increasing the oxidising current in order to accelerate the metal stripping step and in turn to lower the oxygen competition. However, this procedure provokes a significant loss of the detection level since the measurable peak is inversely proportional to the stripping current. A novel solution of removing the oxygen by an electrochemical oxygen filter for the purpose of

omitting the nitrogen purging step has been introduced recently [18,19]. This approach provided a rapid and reliable way of locally removing the oxygen near the sensor surface. It is based on a platinum grid positioned near a sensor surface separated by an isolating porous layer. The application of a given potential at the platinum grid induces the oxygen reduction locally, in the vicinity of the sensor. This approach was successfully studied on the model analyte, paraquat [19] and detection of $NAD(P)^+$ in a biosensing application [18].

In this work, we have applied the developed oxygen filter for the determination of three metals (cadmium, lead, zinc) by SCP. This required a modification of SCP measurement protocols and precise optimization of the used oxygen filter to achieve the complete elimination of oxygen from the area near the surface of the sensor. For this study, a thin mercury film plated on screen-printed electrode [20] was used for SCP experiments. Although the use of mercury is decreasing due to its toxicity, it can be still considered as an excellent electrode material for electroanalytical chemistry [21,22]. Applicability of the optimized SCP was shown by constructing calibration dependencies for all three metals even in their mixtures and by the determination in a model river water sample. The advantages of employing the electrochemical oxygen filter are discussed in relation to the commonly used way of removing oxygen by purging solutions with nitrogen.

2. Materials and methods

2.1 Reagents

The reagents were all of analytical grade and used without further purification. All the solutions used for the experiments were prepared with ultra-pure water (18.2 MΩ cm, Elga labwater). The certified Inductively Coupled Plasma standards of mercury nitrate (1000±4 mg L^{-1}), cadmium nitrate (1000±4 mg L^{-1}), lead nitrate (1000±4 mg L^{-1}) and zinc nitrate (1000±4 mg L^{-1}) as well as the suprapur nitric acid 65% and the sodium hydroxide (100 mM titration standard) were purchased from Fluka. Titrisol buffers (Merck) pH 4, 7 and 10 were used for the daily calibration of the pH electrode. Solutions of sodium nitrate were prepared from the solids (Merck, suprapur). Potassium thiocyanide, hydrochloric acid, potassium chloride and ammonium acetate (all p.a. from Merck) were used to prepare the cleaning solution for the SPE electrode and re-dissolution solution for the mercury film.

2.2 Description of the electrochemical setup

In this work, two three-electrode setups are combined within the same electrochemical cell, as described in the Fig. 1. The first one is dedicated to the metal detection and is composed of a working electrode (a thin mercury film electrode plated on the screen-printed carbon electrode of 3mm diameter (SPE-Hg, WE1 in Fig. 1)), a glassy carbon rod counter-electrode and a Ag/AgCl (in KCl 3M) reference electrode (Dri-Ref5, World Precision Instruments, Sarasota, USA). To apply the electrochemical measurements, the potentiostat/galvanostat Metrohm µAutolab III controlled by the GPES 4.9 software (Ecochemie, The Netherlands) was used. SPEs were kindly provided by C. Parat from the Institut des Sciences Analytiques et de Physico-Chimie pour l'Environnement et les Matériaux (Université de Pau et des Pays de l'Ardour, France). SPEs are described and prepared according to the procedure published [17].

The second setup aims at eliminating the oxygen at the vicinity of the mercury electrode. This electrochemical system comprises: two superposed disk-shaped platinum grids[18,19] as the working electrode (WE2 in Fig.1), a platinum rod as the auxiliary electrode and a Ag/AgCl (in KCl 3M) reference electrode (Dri-Ref5). The Pt grids are sealed off by means of two sheets of insulating adhesive with a pre-cut hole of 5 mm diameter. The connection between the Pt electrode and the setup is achieved by means of carbon fibers, also enclosed between the adhesive strips. A plastic sheet of circa 400 µm of thickness is inserted to allow a safe distance between the Pt grids and the mercury electrode. This setup is connected to an EmStat3+ (Palmsens BV, The Netherlands) and piloted by PStouch software installed on a tablet device that was operating with a battery.

2.3 Preparation of the mercury electrode

The deposition of the thin mercury film on the SPE electrode is repeated daily for each set of experiments with the following step-by-step method [20]. Between each of these steps, the cell is thoroughly cleaned with ultrapure water.

First, the Pt filter electrode is positioned above the SPE electrode, and the electrochemical cell is hermetically sealed and mounted as shown in the Fig. 1. A magnetic stirrer is disposed over the working electrodes and controlled by the 728 Stirrer module from Metrohm.

Then, the SPE electrode is conditioned with an electrochemical pre-treatment using voltammetric scanning (50 cycles) between −0.80V and +0.80V at 0.1 V s^{-1}, in the NH_4Ac (1000 mM)–HCl (500 mM) buffer solution. The thin mercury film is plated ex-situ on the SPE electrode with use of a 0.32 mM mercury (II) nitrate solution under acidic conditions (pH 1.9) via electrodeposition at −1.30 V during 600 s, using the magnetic stirrer at position 1. At this

stage, the mercury electrode SPE-Hg is ready to be used. Once the experiments are completed, the SPE is cleaned by successive mercury reoxidations in 80 mM ammonium thiocyanate solution buffered with ammonium acetate (pH 3.4).

2.4 Experimental protocol for electrochemical metal detection by stripping chronopotentiometry

In this study, the metal is detected by Stripping Chronopotentiometry (SCP). As depicted in Fig. 2, SCP is a two-step technique which comprises: (i) a deposition phase carried out at the specified deposition potential E_d in the limiting current region for a given time and under stirring conditions during a deposition time t_d (ii) a reoxidation process imposed by application of a stripping current, I_s, under unstirred conditions which lasts until the potential reaches a value well past the reoxidation transition plateau. For a planar macroelectrode, the current is generally fixed at 3 µA (42 µA/cm^2) in order to reach the conditions where the amalgamated metal is completely removed from the electrode volume, that is the so-called depletive regime [11]. The resulting electrolysis time allows the quantification of the total accumulated metal. This time is accurately measured by the peak area obtained by the derivative dt/dE vs. E.

In the depletive regime the number of moles deposited during the first step equals:

$$N_{\text{deposited}} = \frac{I_d^* t_d}{nF} \quad (1)$$

where n is the number of exchanged electrons and F the Faraday constant.

And the number of moles reoxidised is given by:

$$N_{\text{oxidised}} = \frac{I_s \tau^*}{nF} \quad (2)$$

where I_s is the stripping current, and τ^* the limiting value for the transition time. The charge balance for complete depletion is given by

$$\tau^* = I_d^* t_d \, / I_s \quad (3)$$

Given that under non-complexing medium, such as acidified solution, we have,

$$I_d^* = \frac{nFAD_M c_{M,T}^*}{\delta} \quad (4)$$

with D_M the diffusion coefficient of M, δ the diffusion layer and $c_{M,T}^*$ the total metal concentration in the bulk solution. We have a direct proportionality relationship between τ^* and $c_{M,T}^*$.

During the stripping process, the amalgamated and reduced metallic form, M^0, can be "chemically" oxidized by traces of oxygen, provoking a competitive oxidation of O_2 which leads to underestimate the total accumulated metal charge proportional to $I_s\tau^*$. Besides, the contribution of the oxygen-derived current on the metal stripping is generally more significant than that of the I_s fed by the galvanostat. This chemical current provokes a fast potential decrease which become more difficult to measure by the electrochemical apparatus. Therefore, the SCP requires a constant oxygen concentration as low as possible during the experimental work. This is generally achieved efficiently by N_2 purging.

When using a thin mercury film electrode, we can apply relatively high reoxidation currents, thus decreasing the oxygen competition by reducing the reoxidation time. Nevertheless, in fully oxygenated solutions, the oxygen concentration is sufficiently high to significantly perturb the measurement. Therefore, it is still necessary to purge the solution for 15-20 minutes and keep an inert gas blanket on top of the sample to continually perform SCP measurements.

2.5 Modified SCP procedure in the presence of the Pt filter

Elimination of oxygen at the vicinity of the SPE-Hg electrode is electrochemically achieved by the O_2 reduction at the Pt working electrode according to the following scheme:

$$O_2 + 4H^+ + 4e^- \leftrightarrow 2H_2O \qquad (5)$$

To carry out the oxygen removal using the Pt electrode in combination with the metal detection, the SCP procedure is slightly modified by splitting the deposition step, t_d, into two substeps. The first substep consists of a deposition phase at the applied potential E_d during $t_{d,s}$ under stirring conditions to ensure facilitated mass transport of the metal from the bulk solution to the electrode. Following this step, the deposition potential is maintained in a quiescent solution to facilitate and optimise the oxygen reduction prior to triggering the stripping process. The duration of this step is given by $t_{d,u}$ (Fig. 2).

The deposition step is carried out at a specified deposition potential E_d of -0.75V for calibrations of Cd or Cd/Pb mixture solutions and of -1.35V for calibrations of Zn/Pb mixture solutions. Then, a 3 µA stripping current i_s is applied for the reoxidation step.

SCP calibrations are performed in 0.1M $NaNO_3$ solution acidified to pH 3, except for experiments involving Zn element for which the pH is fixed at 3.5 to restrict the proton consumption likely occurring at more negative deposition potential and, in turn the eventual local pH change at the vicinity of SPE-Hg electrode.

2.6 Sample preparation for comparison of SCP and IC-PMS

Three samples were prepared to get final metal (Cd, Pb) concentrations of 30 nM. The two first samples were prepared by dilution of Cd and Pb stock solutions (10^4 nM) in ultra-pure water with a final total volume of 50 mL. The first one contains only Cd and the second one is a mixture of Cd and Pb. The 3rd sample was prepared using a river water sample as a natural matrix which was collected in the Orne river in Lorraine (tributary of the Moselle in north eastern France) at the Beth dam site in June 2020. This solution was at first filtered through a filter (Satorius syringe filter 0.2µm pore size cellulose acetate). 50 mL of river water sample was spiked with the stock solutions of 10^4 nM Cd and Pb for a final concentration of 30nM. For the 3 samples, 27 mL of a sample were then diluted to 30 mL with 1M solution of supporting electrolyte $NaNO_3$ (for a final concentration of 100 mM $NaNO_3$) and acidified to pH 3 with 1M nitric acid. Determination was performed by standard addition method using 3 additions at the optimal SCP conditions.

The other parts (23 mL) of the samples were then analysed by ICP-MS. pH of all the samples was adjusted to 1.5 with concentrated nitric acid before the analysis. Determination was performed on the instrument ICP-MS 7800 (Agilent) calibrated with standard solutions of metals in the range 0.1 to 10 ppb, *i.e.* 0.889 to 88.96 nM, 0.483 to 48.26 nM, 1.529 to 152.95 nM, for Cd, Pb and Zn, respectively. The reported concentrations calculated from SCP and ICP-MS techniques correspond to the initial concentrations of the sample, *i.e.* before dilution.

3. Results and discussion

3.1 Evaluation of the Pt grids electrode efficiency to eliminate oxygen

This part is dedicated to reach a sufficient low level of dissolved oxygen with the aid of the Pt filter to moderate O_2 impact on SCP measurements. To do so, the effect of two parameters on the analytical signal is inspected: the potential that has to be applied at the Pt filter electrode, E_{filter}, and the time required during the second substep of the metal deposition, $t_{d,u}$, under no stirring conditions (see Fig. 2).

The current displayed during the deposition step is an experimental indicator of the oxygen content, since this value is driven by the chemical reduction at the Hg electrode surface which corresponds mainly to oxygen. To this end, this current should be as low as possible. In this

section, the produced current at the Hg-plated SPE surface is evaluated by chronoamperometry just after a SCP-like deposition procedure at E_d = -0.75 V for 45 s. Chronoamperometry monitors the time dependence of the current under unstirred conditions, by maintaining the applied potential to -0.75 V. The results are shown in the Fig. 3A.

Two preliminary experiments were investigated in the situation during which the Pt filter was disconnected. In one case, the solution was purged using nitrogen gas during 30 min before measurement. The measured current during the chronoamperometry remains constant around -1 µA, a mean value which is habitually recorded during SCP measurement at E_d = -0.75 V using a thin mercury film electrode in a well-purged solution. Therefore, a current of (-1.0 ± 0.5) µA will be considered here as the reference value for which an acceptable O_2 depleted solution is attained. In the second case, the chronoamperometry is now performed under unpurged conditions. The current decreases with time following a Cottrell-like curve, and limits to a value of -3 µA after 100 s. This finding demonstrates that O_2 reduction occurs at the mercury electrode at -0.75 V. However, the current value, and in turn the oxygen removal, is far from being satisfactory as compared to the N_2 purge scenario.

As depicted in Fig. 3, application of a reductive potential at the Pt filter electrode during the chronoamperometry significantly improves and accelerates the oxygen depletion at the SPE-Hg electrode. Several potentials were applied at the Pt filter electrode in order to find an optimal potential value for oxygen reduction. While for E_{filter}= 0 V, no significant differences are found as compared to the situation where the Pt filter is inoperative under unpurged conditions, for $E_{filter} \leq$ -0.10 V, the current considerably decreases with time, and comparable deoxygenation level of purged solution can be attained at the SPE-Hg electrode's vicinity. Applying more negative potentials at the Pt electrode accelerates the oxygen reduction. However, approaching more negative potential value may cause hydrogen formation at the electrode surface that can probably affect the SCP measurement. Thus, we have opted for a safe reduction potential of E_{filter} = -0.40 V for oxygen removal, which agrees with previous reports [18,19]. Under this condition, a waiting time of 40-50 s is necessary to reach an adequate current of -1.5 µA. Such background value compares well with the -1 µA achieved after 30 min of N_2 purging.

Finally, we have tested the oxygen elimination using the Pt filter at -0.40V under stirring conditions. The result revealed that the current fluctuated around -12 µA, well above the target value. In this particular case, solution convection facilitated the oxygen transport from the bulk solution to the electrode surface, namely O_2 reduction was not rapid enough and less efficient

than in the case of the unstirred solution. We then justified the fact that the deposition step should be split into two stages as detailed in the Fig. 2.

To qualitatively relate the effect of the current reached, and in turn the presence of oxygen, with the final SCP signal, we report the chronopotentiograms for various measured currents, which are obtained by adjusting $t_{d,u}$ values. This evaluation is shown in Fig. 3B. The SCP curves clearly illustrate how oxygen competes in the stripping step, chemically reoxidating the amalgamated metal, thus decreasing the electrochemical signal. For high current values ($|i|$ > 2.0 µA), the baseline is significantly truncated in the range of more negative potential values. For such high current values, this effect originates from an initial fast potential change in the stripping step (see Fig. 2) which cannot be recorded by the potentiostat. The second oxygen effect on SCP measurements is the O_2 contribution in the metal stripping which can severely compete with the applied oxidising current. Thus, the resulting SCP peak area underestimates the amount of amalgamated metal if oxygen content is too high. This effect is partly masked in our results since the amount of metal deposited in the mercury electrode increases with the overall deposition time.

We can see that the baseline is stabilised to a current value of -2.0 µA. On the basis of these overall results, and for a good compromise between an acceptable measurement duration and satisfactory SCP signal, we have fixed the time of the second deposition substep at 45 s, under the application of a potential of -0.40V to the Pt filter in a quiescent solution.

3.2 Impact of the oxygen elimination system on Cd detection limits using SCP technique

The detection and quantification limits are evaluated by performing Cd calibrations using several oxygen elimination systems. The results, including the limit of detection and quantification, are gathered in the table 1.

The values of LOD and LOQ are estimated from the calibration curves according to this equation:

$$LOD = 3\ Sy/m \quad (6.a)$$

$$LOQ = 10\ Sy/m \quad (6.b)$$

where Sy is the standard deviation of the residuals and m is the slope of the calibration plot [23].

Two calibrations were elaborated after a 30 min nitrogen purge in the solution. Under this condition, we obtained LOD which were comparable to those measured for a same type of electrode and SCP procedure [20] in a different cell which ranged from 3.6 to 9.6 nM for a deposition time of 45 s. Note that the slightly higher LOD value found in our study can arise from a less efficient mass transport due to the arrangement of our electrochemical cell. Our SPE-Hg electrode is positioned on the bottom of a well, while in the study of Monteiro *et al* [24] the electrode is directly immersed in the solution. The LOD can be improved by changing the deposition time $t_{d,s}$. For example, the LOD is two times lower if $t_{d,s}$ is extended from 45 to 90 s, as can be derived from the relationship of the Eq. (6.a).

The presence of oxygen dramatically impacts on the LOD threshold, Cd is not perfectly detected below a concentration of 100 nM. The O_2 elimination by using the mercury electrode and prolonging the deposition substep with the unstirred period helps to significantly decrease the LOD value under a reasonable threshold. The coupled use of SCP with the Pt filter provides comparable LOD results than those obtained with nitrogen purging. This finding confirms the high efficiency of the oxygen removal process by the platinum electrode and this validates the preceding conclusions obtained by chronopotentiometry.

We also stress out, from our experimental observations, that the control of deoxygenation level for the whole duration of the experiments is of major importance. Keeping the nitrogen blanket during several hours can lead to a slow decrease of the bulk oxygen concentration upon time, and in turn, this may also modify the stripping conditions. This is particularly required to stabilise in the best possible way the level of oxygen content from the elaboration of the calibration until the metal quantification procedure. The use of Pt filter seems to offer a good stabilisation of the level of oxygen for each SCP measurement.

As an illustration, we have recorded the current value which is displayed at the final stage of the deposition step for over 25 measurements (2 hours) under nitrogen purging conditions and under Pt filter effect. Over that period, the current value generally decreased from -1.0 to -0.5 µA under N_2 purging, whereas the current was kept constant around a value of (0.9 ± 0.1) µA when the filter was used. Therefore, the O_2 removal driven by the Pt filter is fully reproducible from the first measurement to the very last. Additionally, it also stabilises the conditions under which the stripping step is performed.

3.3 Zn, Cd and Pb detection

In the present section, the metal detection is extended to other elements than cadmium such as lead and zinc. We have performed a series of calibrations that combined the quantification of the Cd and Pb couple (Fig. 4A&B), and another one with Zn and Pb (Fig. 4C&D).

For the first set of data, the results for cadmium are not shown as LOD/LOQ are very similar to those given in Table 2. The detection limits for lead are comparable to those obtained for cadmium. However, for Pb element, we observe a loss of linearity of the calibration dependence starting at a concentration above 100 nM, due to its lower solubility in mercury compared to cadmium or zinc [25].

Detection of the both zinc and lead are shown in Fig. 4C&D. The LOD pertaining to the SCP detection of zinc is higher than those of lead and cadmium but calibration dependence displays a satisfactory linear regression. Note that SCP performed at the deposition potential of zinc affects the baseline, particularly in the vicinity of peaks of Pb. However, this does not affect the calibration dependence quality if the peak area is measured, and a simple baseline correction can be applied.

As mentioned before, mass transport towards the mercury electrode is not optimized due to the configuration of the electrochemical cell since the two-electrode setup is positioned at the bottom of a well. To improve the analytical sensitivity, the two electrodes could be integrated in a wall-jet electrochemical flow cell, that would significantly improve the fluid hydrodynamics. In these conditions, as reported in Figure 2, the protocol will integrate a short period without wall-jet flow before stripping analysis.

3.4 Dosing Cd and Pb in model samples and samples of river water

In order to evaluate the application of the proposed method for total metal quantification in solution, we have prepared three model samples. These three tested solutions were spiked with concentrated solutions of Cd and Pb, then the content of metals was evaluated by the standard addition method by SCP. Because of the possible matrix effects, a quadratic fit [26] is used to determine the concentration of metals in the river water sample. We have found an acceptable match between expected values and found values by SCP confirming the applicability of the proposed method for real samples. Note that a low content of lead in the river water solution is found by ICP-MS. This may result from the different metal quantification approach employed for ICP-MS and SCP. While standard additions were adopted for electrochemistry measurements, ICP-MS were performed using a calibration curve for which the matrix effects are disregarded. The results are summarized in Table 3.

4. Conclusion

In this work we have presented a novel procedure of the oxygen removal from the solution. This has been presented for SCP technique that is exceptionally sensitive to oxygen. The proposed oxygen elimination system offers a quick, reliable and reproducible removal of oxygen in the vicinity of the working electrode. We have proven that by application of a negative potential (-0.40 V) at the Pt grid, it is possible to sufficiently remove oxygen near the electrode surface, under unstirred conditions. SCP measurement protocols had to be modified accordingly. The deposition step was split in two stages, which were differed by the presence of stirring. Calibration curves were obtained for three metals Cd, Pb and Zn at the SPE-Hg with detection limits in nanomolar level, similar to LOD obtained under nitrogen atmosphere. Detection limits should be improved by using longer deposition times or by modifying the electrochemical cell design to improve the mass transport at the electrode, e.g. by using a wall-jet flow cell. This work provides a robust basis to more applications of the oxygen filter system dedicated to other stripping-based technique as AGNES (Absence of Gradients and Nernstian Equilibrium Stripping) for the detection of metal free ions in solution. Moreover, the working electrode can be easily exchanged for other screen-printed electrodes or their modifications as the use of mercury electrodes is decreasing in favour of modified screen-printed electrodes based on gold, bismuth, antimony or tin [27]. In addition, application of oxygen filter significantly improves the usefulness of the analytical system for the on-site analysis.

Acknowledgments. We acknowledge the support of the French INSU/EC2CO program for the 2017-2019 period. JPP and ER acknowledge the financial support of the European Union's Horizon 2020 Research and Innovation Programme under the Grant Agreement No. 776804 — H2020-SC5-2017 (project acronym NEXT). JG acknowledges SATT Sayens for financial support. Claire Genois is acknowledged for ICP-MS measurements and Hela Smati for the preliminary results she obtained during her master training.

References

[1] G.F. Nordberg, B.A. Fowler, M. Nordberg, Handbook on the Toxicology of Metals, Academic Press, 2014.
[2] J. Buffle, Complexation reactions in aquatic systems: an analytical approach, E. Horwood, Chichester, 1988.

[3] A.J. Borrill, N.E. Reily, J. V. Macpherson, Addressing the practicalities of anodic stripping voltammetry for heavy metal detection: A tutorial review, Analyst. 144 (2019) 6834–6849. https://doi.org/10.1039/c9an01437c.
[4] A. Kumar, A.L. Ramanathan, M.B.K. Prasad, D. Datta, M. Kumar, S.M. Sappal, Distribution, enrichment, and potential toxicity of trace metals in the surface sediments of Sundarban mangrove ecosystem, Bangladesh: a baseline study before Sundarban oil spill of December, 2014, Environ. Sci. Pollut. Res. 23 (2016) 8985–8999. https://doi.org/10.1007/s11356-016-6086-6.
[5] G.O. Duodu, A. Goonetilleke, G.A. Ayoko, Comparison of pollution indices for the assessment of heavy metal in Brisbane River sediment, Environ. Pollut. 219 (2016) 1077–1091. https://doi.org/10.1016/j.envpol.2016.09.008.
[6] J.S. Barin, P.A. Mello, M.F. Mesko, F.A. Duarte, E.M.M. Flores, Determination of elemental impurities in pharmaceutical products and related matrices by ICP-based methods: a review, Anal. Bioanal. Chem. 408 (2016) 4547–4566. https://doi.org/10.1007/s00216-016-9471-6.
[7] E. Companys, J. Galceran, J.P. Pinheiro, J. Puy, P. Salaün, A review on electrochemical methods for trace metal speciation in environmental media, Curr. Opin. Electrochem. 3 (2017) 144–162. https://doi.org/10.1016/j.coelec.2017.09.007.
[8] B. Bansod, T. Kumar, R. Thakur, S. Rana, I. Singh, A review on various electrochemical techniques for heavy metal ions detection with different sensing platforms, Biosens. Bioelectron. 94 (2017) 443–455. https://doi.org/10.1016/j.bios.2017.03.031.
[9] H. van Leeuwen, R. Town, Stripping chronopotentiometry at scanned deposition potential (SSCP). Part 1. Fundamental features, J. Electroanal. Chem. 536 (2002) 129–140. https://doi.org/10.1016/S0022-0728(02)01212-3.
[10] R.M. Town, H.P. van Leeuwen, Stripping chronopotentiometry at scanned deposition potential (SSCP): Part 2. Determination of metal ion speciation parameters, J. Electroanal. Chem. 541 (2003) 51–65. https://doi.org/10.1016/S0022-0728(02)01314-1.
[11] R.M. Town, H.P. van Leeuwen, Fundamental features of metal ion determination by stripping chronopotentiometry, J. Electroanal. Chem. 509 (2001) 58–65. https://doi.org/10.1016/S0022-0728(01)00420-X.
[12] E. Rotureau, P. Pla-Vilanova, J. Galceran, E. Companys, J.P. Pinheiro, Towards improving the electroanalytical speciation analysis of indium, Anal. Chim. Acta. 1052 (2019) 57–64. https://doi.org/10.1016/j.aca.2018.11.061.
[13] D. Jedryczko, P. Pohl, M. Welna, Determination of the total cadmium, copper, lead and zinc concentrations and their labile species fraction in apple beverages by flow-through anodic stripping chronopotentiometry, Food Chem. 225 (2017) 220–229. https://doi.org/10.1016/j.foodchem.2016.12.092.
[14] C. Parat, L. Authier, A. Castetbon, D. Aguilar, E. Companys, J. Puy, J. Galceran, M. Potin-Gautier, Free Zn2+ determination in natural freshwaters of the Pyrenees: towards on-site measurements with AGNES, Environ. Chem. 12 (2015) 329. https://doi.org/10.1071/EN14184.
[15] R.M. Town, H.P. van Leeuwen, Stripping chronopotentiometry at scanned deposition potential (SSCP): An effective methodology for dynamic speciation analysis of nanoparticulate metal complexes, J. Electroanal. Chem. 853 (2019). https://doi.org/10.1016/j.jelechem.2019.113530.
[16] R.M. Town, H.P. van Leeuwen, Fundamental features of metal ion determination by stripping chronopotentiometry, J. Electroanal. Chem. 509 (2001) 58–65. https://doi.org/10.1016/S0022-0728(01)00420-X.
[17] C. Parat, A. Schneider, A. Castetbon, M. Potin-Gautier, Determination of trace metal speciation parameters by using screen-printed electrodes in stripping

chronopotentiometry without deaerating, Anal. Chim. Acta. 688 (2011) 156–162. https://doi.org/10.1016/j.aca.2010.12.034.
[18] T.X.H. Le, M. Etienne, F. Lapicque, A. Hehn, N. Vilà, A. Walcarius, Local removal of oxygen for NAD(P)+ detection in aerated solutions, Electrochimica Acta. 353 (2020) 136546. https://doi.org/10.1016/j.electacta.2020.136546.
[19] M. Etienne, T.X.H. Le, T. Nasir, G. Herzog, Electrochemical Filter To Remove Oxygen Interference Locally, Rapidly, and Temporarily for Sensing Applications, Anal. Chem. 92 (2020) 7425–7429. https://doi.org/10.1021/acs.analchem.0c00395.
[20] S.C.C. Monterroso, H.M. Carapuça, J.E.J. Simão, A.C. Duarte, Optimisation of mercury film deposition on glassy carbon electrodes: evaluation of the combined effects of pH, thiocyanate ion and deposition potential, Anal. Chim. Acta. 503 (2004) 203–212. https://doi.org/10.1016/j.aca.2003.10.034.
[21] A. Economou, P.R. Fielden, Mercury film electrodes: developments, trends and potentialities for electroanalysis, Analyst. 128 (2003) 205–213. https://doi.org/10.1039/B201130C.
[22] J. Gajdar, E. Horakova, J. Barek, J. Fischer, V. Vyskocil, Recent Applications of Mercury Electrodes for Monitoring of Pesticides: A Critical Review, Electroanalysis. 28 (2016) 2659–2671. https://doi.org/10.1002/elan.201600239.
[23] E.R. Ziegel, Statistics and Chemometrics for Analytical Chemistry, Technometrics. 46 (2004) 498–499. https://doi.org/10.1198/tech.2004.s248.
[24] A.S.C. Monteiro, C. Parat, A.H. Rosa, J.P. Pinheiro, Towards field trace metal speciation using electroanalytical techniques and tangential ultrafiltration, Talanta. 152 (2016) 112–118. https://doi.org/10.1016/j.talanta.2016.01.053.
[25] F. Vydra, K. Štulík, E. Juláková, Electrochemical Stripping Analysis, E. Horwood, Chichester, West Sussex, UK, 1976.
[26] G.R. Bruce, P.S. Gill, Estimates of Precision in a Standard Additions Analysis, J. Chem. Educ. 76 (1999) 805. https://doi.org/10.1021/ed076p805.
[27] A. Economou, Screen-printed electrodes modified with “green” metals for electrochemical stripping analysis of toxic elements, Sens. Switz. 18 (2018). https://doi.org/10.3390/s18041032.

Figures and Tables

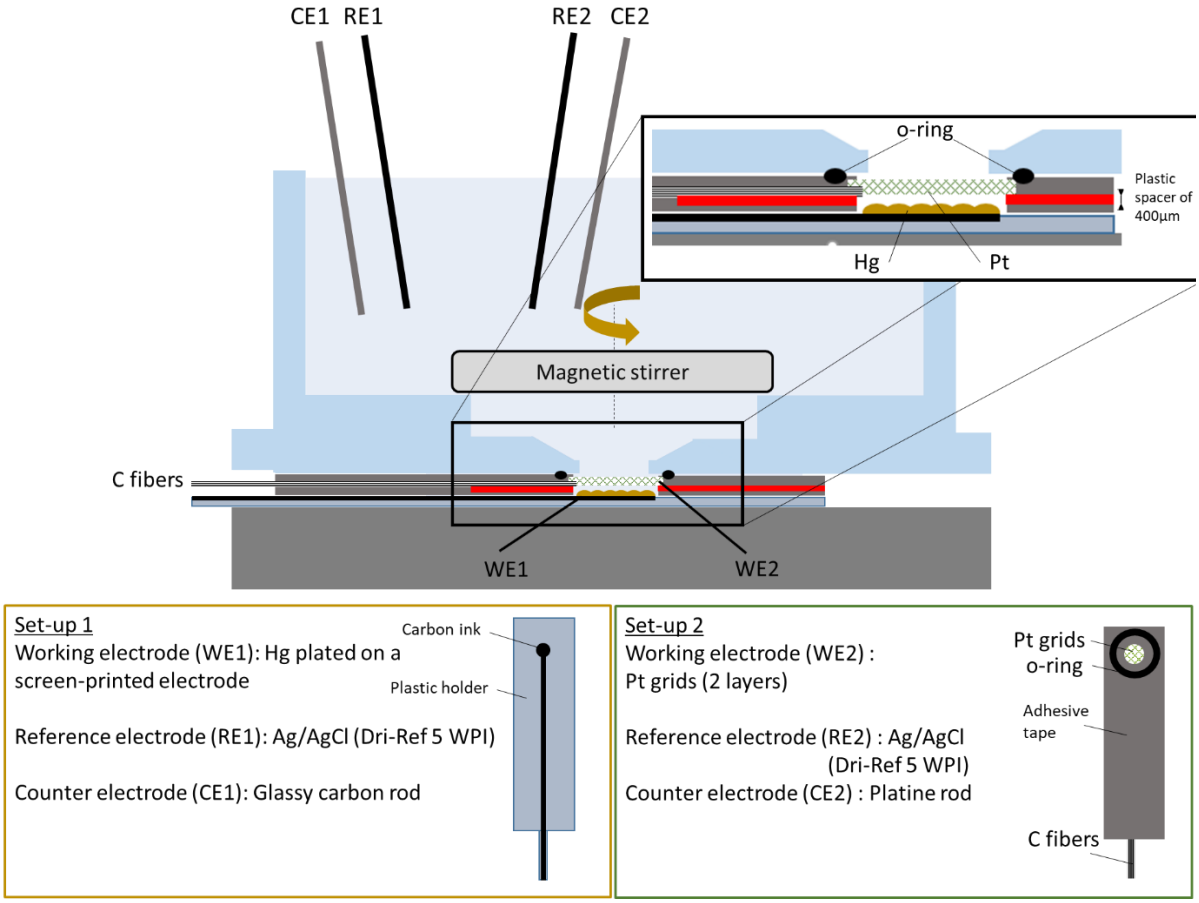

Figure 1: Electrochemical setup including the metal detection system with the mercury film electrode (working electrode n°1, WE1) and the oxygen elimination technique using the platinum electrode (working electrode n°2, WE2). More details are given in the main text.

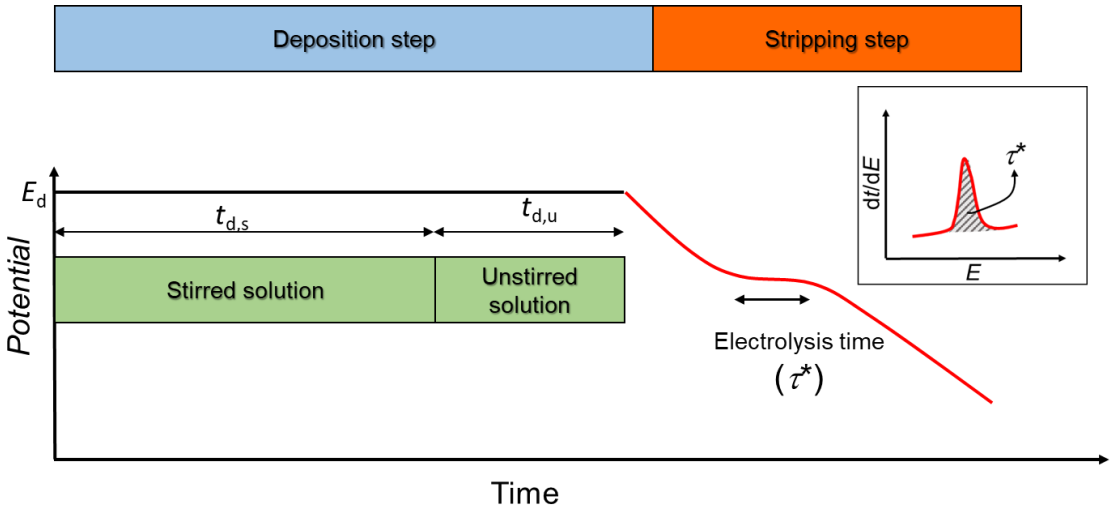

Figure 2: Modified procedure of stripping chronopotentiometry in combination with the oxygen reduction at the Pt filter electrode. SCP measurements are conducted with $t_{d,s}$ the deposition time under stirring conditions fixed at 45 or 90s and $t_{d,u}$ the deposition time without stirring at 45s. The deposition potential is E_d=-0.75V for Cd and Pb detection and -1.35V for Zn detection. The Pt filter is activated during all SCP steps.

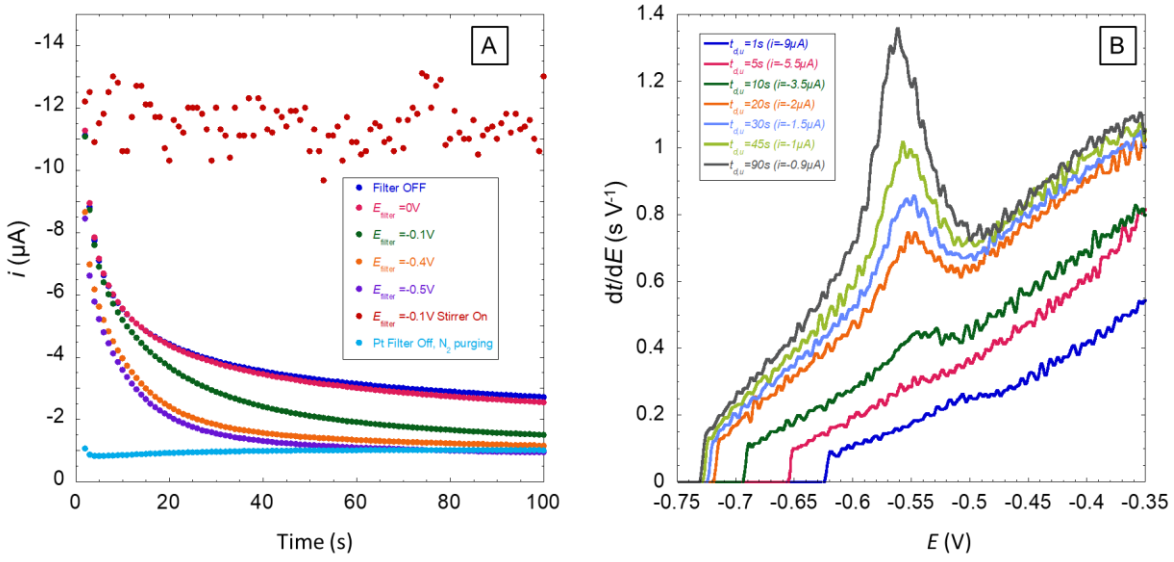

Figure 3: (A) Chronoamperograms at the mercury electrode (WE1) obtained after a deposition potential of E_d=-0.75 V applied during 45 s, to mimic the SCP procedure. The potential at the WE1 is maintained at E_d=-0.75 V under different conditions. The Pt filter (WE2) is inactive, the solution is unstirred with (a) no N_2 purging and (b) after 30min of N_2 purging. The Pt filter is active in an unpurged and quiescent solution at different applied potentials (c) E_{filter} = 0V, (d) E_{filter} = -0.10V, (e) E_{filter} = -0.40V, (f) E_{filter} = -0.50V and (g) under stirring conditions with E_{filter} = -0.10V. Experiments are performed in a 100 mM

$NaNO_3$ solution at pH 3, in absence of metal ions. (B) SCP results for Cd ions as a function of the measured current *i* as read after different $t_{d,u}$ of (a) 1s (*i*=-9.0µA), (b) 5s (*i*=-5.5µA), (c) 10s (*i*=-3.5µA), (d) 20s (*i*=-2.0µA), (e) 30s (*i*=-1.5µA), (f) 45s (*i*=-1.0µA), (g) 90s (*i*=-0.9µA). The SCP are obtained using a deposition potential of -0.75 V. Experiments are performed in a solution of 100 mM $NaNO_3$ at pH 3.00 containing a total Cd concentration of 66 nM.

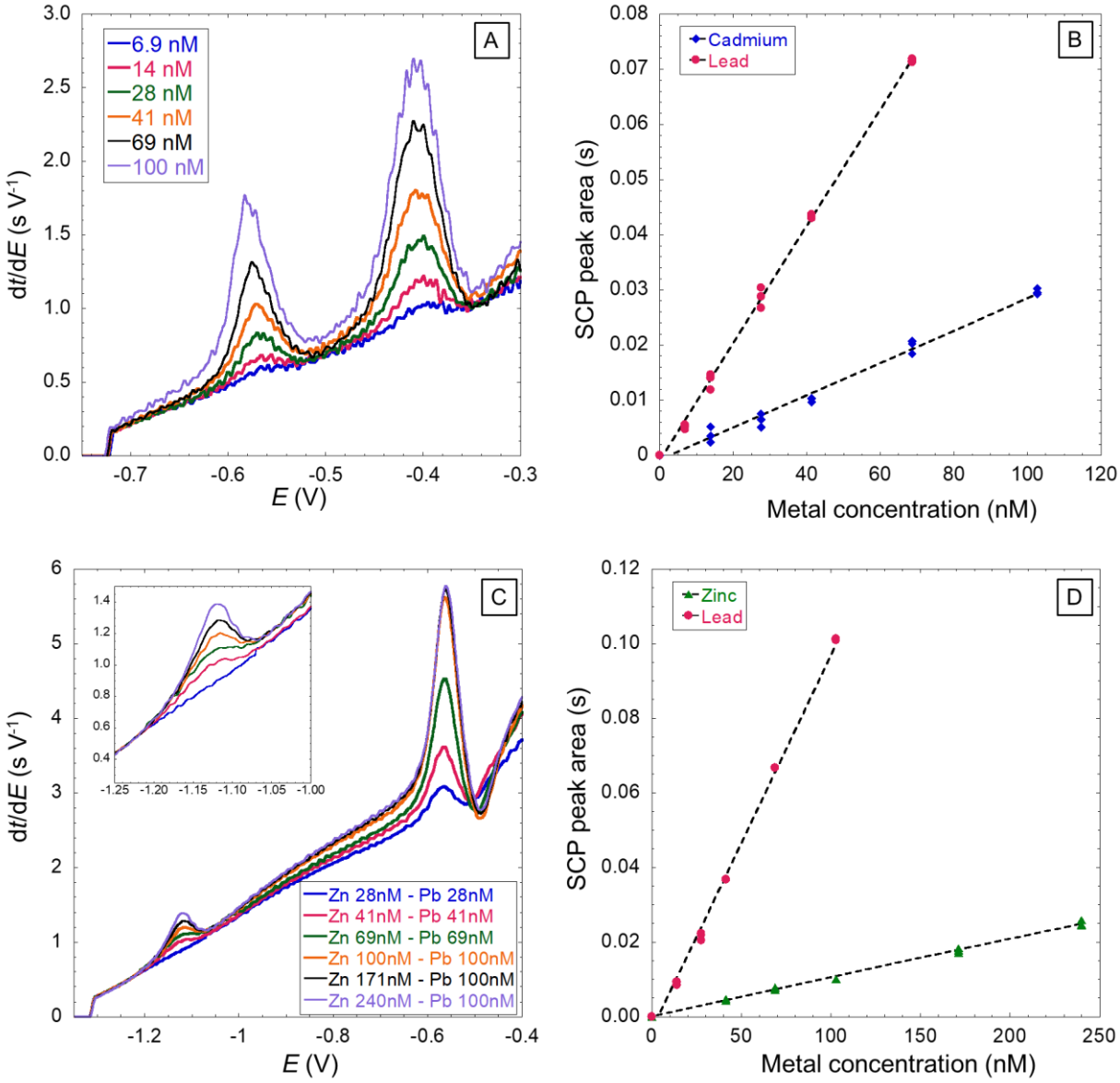

Figure 4: Chronopotentiograms obtained for calibrations of the mixtures Cd, Pb (A) and Zn,Pb (C) and the corresponding calibration curves for couples Cd, Pb (B) and Zn, Pb (D). Experiments were performed in the 100 mM $NaNO_3$ solution at pH 3.0 (for Cd and Pb) or at pH 3.5 (for Zn and Pb) with potential -0.4V applied to the Pt filter.

Range of Cd concentrations nM	Deposition procedure			Calibration					
	$t_{d,s}$ (s)	$t_{d,u}$ (s)	Purging system	*m* (s nM^{-1})	*b* (s)	Sy	LOD (nM)	LOQ (nM)	Lowest detected concentration (nM)
7-100	45	1	N_2	4.3×10^5	1.1×10^{-3}	1.6×10^{-3}	11.1 ± 1	37.1± 3	7
7-100	90	1	N_2	8.5×10^5	1.4×10^{-3}	1.45×10^{-3}	5.1 ± 0.5	17.0 ±2	7
7-100	45	1	None	-	-	-	>100	>100	70
7-100	45	45	None	2.75×10^5	-8.5×10^{-4}	1.3×10^{-3}	15 ± 2	50.0 ± 7	30
7-100	45	45	Pt Filter	3.7×10^5	-9.3×10^{-3}	1.3×10^{-3}	10.6 ± 1	35.6 ± 3	14
7-100	90	45	Pt Filter	4.8×10^5	-1.4×10^{-3}	1.4×10^{-3}	7.5 ± 0.5	25.0 ± 2	7
7-100	90	45	Pt Filter	4.8×10^5	-0.6×10^{-4}	9.8×10^{-4}	6.1 ± 0.5	20.3± 1	7

Table 1. Limits of detection (LOD) and quantification (LOQ) derived from Cadmium calibrations and obtained for different oxygen removal system, performed in Cd containing solution of $NaNO_3$ 100 mM. *m* is the slope, *b* is the intercept, Sy is the standard deviation of residuals. The values of the lowest detected concentrations indicate the concentrations of the first samples which can be measured and used for the calibration plots.

Range of metal concentrations nM	Metal	Deposition procedure		Calibration				
		t_d (s)	E_d (V)	*m* (s nM^{-1})	*b* (s)	Sy	LOD (nM)	LOQ (nM)
7-100	Cd (with Pb)	45	-0.75	1.5×10^5	3.35×10^{-5}	6.4×10^{-4}	12.8± 1	42.7± 3
7-100	Cd (with Pb)	45	-0.75	3.05×10^5	-1.2×10^{-3}	1.13×10^{-3}	13.3± 1	44.4± 3
7-100	Cd (with Pb)	90	-0.75	4.8×10^5	-0.6×10^{-4}	9.8×10^{-4}	6.1 ± 0.5	20.3± 1
7-100	Pb (with Cd)	90	-0.75	5.62×10^5	-1.4×10^{-3}	1.41×10^{-3}	12.5± 1	41.5± 3
7-100	Pb (with Cd)	45	-0.75	5.8×10^5	-2.2×10^{-4}	2.3×10^{-3}	11.9 ± 1	39.8 ± 3
7-100	Pb (with Cd)	45	-0.75	6.1×10^4	-1.1×10^{-3}	2.7×10^{-3}	13.2± 0.5	44.1 ± 2
7-100	Pb (with Cd)	90	-0.75	1.1×10^6	-9.3×10^{-4}	2.2×10^{-3}	6.2 ± 0.5	20.7 ± 2
7-100	Pb (with Cd)	90	-0.75	8.7×10^5	-2.6×10^{-3}	2.8×10^{-3}	9.6 ± 1	31.8 ± 3
40-100	Pb (with Zn)	90	-1.35	1.3×10^6	-4.7×10^{-4}	3.0×10^{-3}	7.0 ± 0.5	23.5 ± 2
40-100[a]	Pb (with Zn)	90	-1.35	1.0×10^6	-3.9×10^{-3}	2.5×10^{-3}	7.5 ± 1	25.0 ± 3
40-100 [a]	Zn (with Pb)	90	-1.35	1.0×10^5	6.9×10^{-5}	5.1×10^{-4}	14.8± 1	49.5 ± 3
40-800	Zn (with Pb)	90	-1.35	3.4×10^5	4.6×10^{-4}	1.7×10^{-3}	15.2± 1.5	50.7± 5

Table 2. Limits of detection (LOD) and quantification (LOQ) derived for a several calibrations of Cd, Pb and Zn calibrations in solution of $NaNO_3$ 100 mM at pH 3.00, except for ([a]) done at $NaNO_3$ 20 mM pH 3.50. *m* is the slope, *b* is the intercept, Sy is the standard deviation of residuals.

Matrix	Expected, nM		Found by SCP, nM		Found by ICP-MS, nM	
	Cd	**Pb**	**Cd**	**Pb**	**Cd**	**Pb**
Deionised water	30	-	31.3±9.5	-	29.44±0.47	-
Deionised water	30	30	23.0±4.5	28.4±4.2	30.24±0.66	26.74±0.88
River water	30	30	26.1±7.2	27.0±7.6	25.62±0.26	16.41±0.23

Table 3. Determination of concentration of Cd and Pb in deionised water samples and the river water sample by standard addition method by SCP and by ICP-MS.

Graphical abstract